Wheaton Journal of
Neurobiology Research

Issue 10, Fall 2017:

"Modeling disease using primary neuronal tissue culture"

R.L. Morris, Editor. Wheaton College, Norton, Massachusetts.

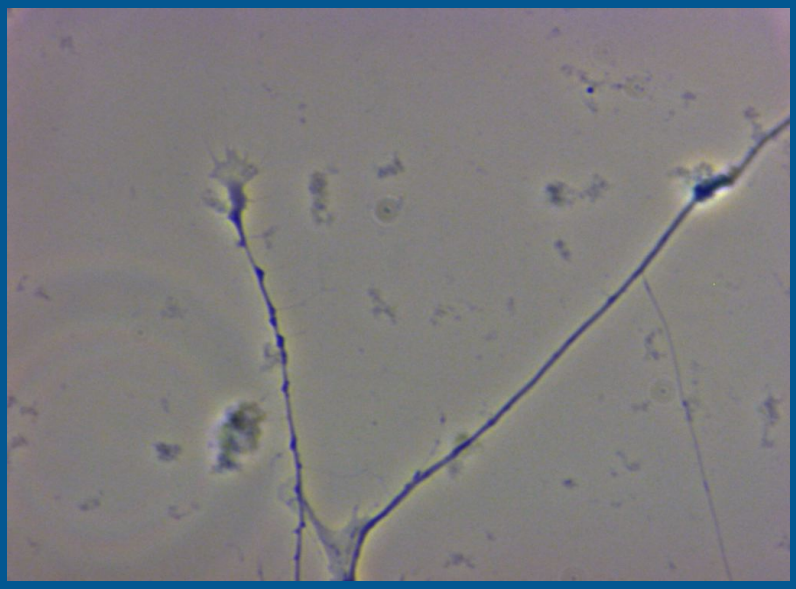

A preliminary observation of neuroprotective effects of k252a on axonal outgrowth in *Gallus gallus* neurons exposed to amyloid-ß

Nathaniel G. Awkerman

BIO 324 / Neurobiology
Final Research Paper
4 December 2017

A preliminary observation of neuroprotective effects of k252a on axonal outgrowth in *Gallus gallus* neurons exposed to amyloid-ß

Nathaniel G. Awkerman
Final Research Paper written for
Wheaton Journal of Neurobiology Research
BIO 324 / Neurobiology
Wheaton College, Norton Massachusetts
4 December 2017

Introduction

Despite being the most prevalent neurodegenerative disease, there is currently an incomplete understanding of the pathology of Alzheimer's disease and how to potentially treat the cause rather than the symptoms (Perl 2010). One of the main causes of neurodegeneration in Alzheimer's patients is the development of NFTs (Neurofibrillary Tangles) that are composed of hyperphosphorylated tau, a microtubule stabilization protein (Serrano-Pozo et al., 2011). NFTs are often found in high density alongside a high concentration of Amyloid-ß precursor protein aggregates (Serrano-Pozo et al., 2011; Brion, 1998). While some of the mechanisms associated with the development of NFTs are known, it is still unclear how the many proposed factors contribute to a complete mechanism. This incomplete understanding coupled with the issue that Alzheimer's generally arises in tandem with other neurodegenerative symptoms, makes the cause of Alzheimer's disease difficult to determine due to potential coexistent conditions (Perl 2010). Axonal degradation will be the focus of this study as it is often a key sign of NFT formation due to reduced microtubule stability from misfolded tau, (Serrano-Pozo et al., 2011). Specifically, this study aims to analyze the impact of exogenous amyloid beta on the axonal growth of embryonic neurons in culture, as well as a possible neuroprotective compound that acts on tau associated kinases to alleviate symptoms of neurodegeneration.

Amyloid-ß plaques, particularly those produced by aggregation of $Aß_{1-40}$, can cause site-specific phosphorylation of tau along its tubulin-binding domain through the activation of several kinases including mitogen-activated protein kinases and glycogen synthase kinase 3 beta (Zheng et al., 2002). (Zheng et al., 2002) also tested aggregation of $Aß_{25-35}$ and showed comparable results for both fragment 25-35 and 1-40. This study will use fragment 25-35 instead of the more common aggregates in Alzheimer's patients, fragments 1-40 and 1-42, as it produces analogous results and is still present in Alzheimer's pathogenesis (Murphy et al., 2010). The kinase PKN is redistributed to neurites and cortical cytoplasm instead of its typical site of congregation, the endoplasmic reticulum, in neurons afflicted by Alzheimer's disease and its over-activity may lead to the formation of NTFs (Kawamata et al., 1998). PKN also has several phosphorylation sites along the microtubule-binding domain of Tau proteins along the C-terminus. PKN is able to phosphorylate Ser-258, Ser-320, and Ser-352, and, while a majority of PKC/PKN family kinases can phosphorylate Ser-258 and Ser-352, the phosphorylation of Ser-320 along the microtubule-binding domain is unique to PKN (Taniguchi et al., 2000). Highly potent and cell permeable kinase inhibitor k252a has been shown to reduce phosphorylation from PKC and PKN family

kinases among others and also provides protective effects to neurons in culture (Kase et al., 1987; Roux et al., 2002). It is hypothesized that kinase inhibitor k252a may provide neuroprotective effects by conserving positive axonal outgrowth in cultured cells if axonal retraction is triggered in neurons due to neurotoxic effects from exposure to $Aß_{25-35}$.

For this study, peripheral neurons of embryonic *Gallus gallus* were used, specifically the dorsal root ganglia. This is due to the ease of extraction via dissection and plating, general availability, and the organism's extensive history as a model organism for disease pathogenesis in vertebrates (Burt 2007). Cultures grown to 2 days will be used to study axonal outgrowth in vitro. Two experimental conditions were established: $Aß_{25-35}$ and k252a with $Aß_{25-35}$, to establish a model of neurodegeneration and test for protective effects of k252a.

Materials and Methods

Materials:

For the control condition, amyloid-ß fragment 35-25 (Sigma Aldrich catalog number A2201) in DMSO was added to control for the addition of peptide and DMSO in experimental conditions. $Aß_{35-25}$ is composed of the same amino acids as the experimental condition, just in a reverse order rendering it inactive (Hedin et al., 2001). In experimental conditions, amyloid-ß 25-35 (Sigma Aldrich catalog number A4559) was used to model Alzheimer's pathogenesis and kinase inhibitor k252a (Santa Cruz Biotechnology catalog number sc-200517) was tested as a potentially neuroprotective compound.

Following Dr. Morris' procedure, the dorsal root ganglia of *Gallus gallus* were dissected, minced, and plated while some remaining ganglia were triturated and plated in low density in conjunction with minced ganglia (Morris, 2015a). Cells were plated in 2ml of F-plus medium on glass 22x22mm coverslips cleaned in 70% EtOH and treated with poly-lysine and laminin and allowed to grow for 2 days at 37˚C.

Imaging was performed through the Wheaton College Imaging Center for Undergraduate Collaboration (ICUC) with a Nikon-E200 microscope equipped with a Sony DFW-X700 camera connected via a C-mount with 1x magnification. Data was collected through the BTV software program, version 6.0b1, on iMac computers running OS X Yosemite version 10.10.5. All images were taken at 40x magnification with optics set to phase ring 2.

Culture preparation:

While the cultures were being prepared, a 2.5mM stock solution of amyloid-ß 25-35 was created two days prior to use by adding 377µl of sterile DMSO to 1mg of peptide. Amyloid-ß 35-25 control stock was similarly created at 2.5mM by adding 94µl of sterile DMSO to 250µg of peptide while the k-252a stock solution was created at 1mM in a fume hood due to potentially toxic effects by adding 214µl of sterile DMSO to 100µg of solid. Additionally, 2µl of k252a 1mM stock solution was added to 198µl of sterile DMSO for a 1:100 serial dilution resulting in a working solution of 10µM. All stock and working solutions were stored at -20˚C while the k-252a solutions were also wrapped in tin foil to prevent light exposure.

One hour prior to growth medium exchange, working solutions were prepared using six 1ml aliquots of F-plus growth medium. For the control condition, 10µl of 2.5mM amyloid-ß 35-25 stock was added to 1ml of growth medium for a working concentration of 25µM to match the experimental dosage. Similarly, in the strictly amyloid-ß treatment, 10µl of 2.5mM amyloid-ß 25-35 stock was added to 1ml of growth medium for a working concentration of 25µM. A 25µM concentration of Amyloid-ß 25-35 was chosen as it produces neurotoxic effects analogous to

Alzheimer's pathology in primary neurons at that dosage (Lattanzio et al., 2016). Finally for the amyloid-ß and k252a treatments, 10µl of 2.5mM amyloid-ß 25-35 stock and 10µl of 10µM k252a working solution were added to 1ml of growth medium resulting in final working concentrations of 25µM and 100nM respectively for that level of treatment. A nanomolar concentration of k252a was used in this study as k252a has been shown to provide neuroprotective effects in concentrations up to 200nM and neurotoxic effects in larger concentrations (Roux et al., 2002). 2ml of growth medium was then removed from each culture dish and exchanged with the prepared working solutions resulting in a control and two levels of treatment totaling 3 culture dishes as there were no biological replicates. The cultures were then allowed to incubate for 24 hours at 37˚C before imaging.

Chip Chamber Preparation:

After the 24-hour incubation period, chip chambers were prepared by placing a square perimeter of glass coverslip shards in the center of a glass microscope slide slightly smaller than a 22x22 mm coverslip. One to three droplets of growth medium from the culture dishes were then placed in the center of the glass chip perimeter. Growth medium was then pipetted off the culture dish until the level dropped below the top of the treated coverslip but not below the bottom of it. Sharp forceps were then used to tease up the coverslip from the culture dish and the coverslip was inverted, cell side down, and placed on top of the glass chip perimeter at an angle to allow the droplets of growth medium to cover the underneath of the coverslip to prevent dehydration. The coverslips were then sealed onto the glass slides and against contact with the air using heated valap to cover each of the edges. Salts from the growth medium were then washed from the top of the cover slip. This was all according to a procedure developed by Dr. Morris (Morris, 2015b).

Imaging:

All chip chambers were heated to a range of 35-37˚C during data collection to observe dynamic movement using a space heater aimed at the microscope stage and monitored with a temperature sensor placed on the stage. One axon was measured in the one control condition while two axons were imaged in both the amyloid-ß condition and k252a condition. Conditions were imaged every 30 seconds after a 2 minute initial warming period at phase 2, 40x magnification.

Quantification:

Data was analyzed using the Fiji program version 1.0 to measure pixel distances between images. First, scale bars were established by imaging a ruler attached to a glass slide at 4x magnification to determine how many pixels equated to millimeter on each computer. The ruler fragment was measured from the end of one black bar to the end of another black bar for a total of 625 pixels. If 1mm is equivalent to 625 pixels at 4x magnification, it was calculated that 100µm is also equivalent to 625 pixels at 40x magnification, which equals 6.25 pixels per micron.

For the each measured axon, the start of a line segment in Fiji was placed in the estimated center of the lamellipod. Filopodial projections smaller than 2 microns in width were ignored when measuring lamellipodial dimensions for estimation due to their dynamic nature. The images were then analyzed sequentially until the final image where the end of the line segment would be placed at the center of the lamellipod in that image. This distance was then measured in

pixels using the Measure command and converted into microns using the scale conversion above. Any lengthening of the axon was counted as growth and measured as a positive value while any shortening was considered to be retraction and was counted as a negative value. When view field shifted due to axons moving out of frame, identical view fields were quantified and data was summed to determine distance traveled. Once the raw pixel distances were converted to microns, the data was then normalized to microns per minute due to the different durations of data collection between levels of treatment.

Results

Figures 1 through 3 show the development of the observed neurons over a brief period of time qualitatively showing the effects of amyloid-ß on hindering axonal development in 2-day cultured neurons. Figure 1 documents normal axonal outgrowth of cultures treated with the amyloid-ß control fragment. While the growth cones displayed in the control and k252a levels of treatment visibly extend, the amyloid-ß level of treatment shows retractile action affecting the distal axon, beginning with a reduction in the size of the growth cone. This is shown clearly in Figure 2 and the gathering of phase dense structures within the axon can be observed. Figure 3 shows neurons treated with amyloid-ß 25-35 and with k252a. While a large amount of protein aggregates can be seen in Figure 3, they do not seem to induce retraction as shown in Figure 2.

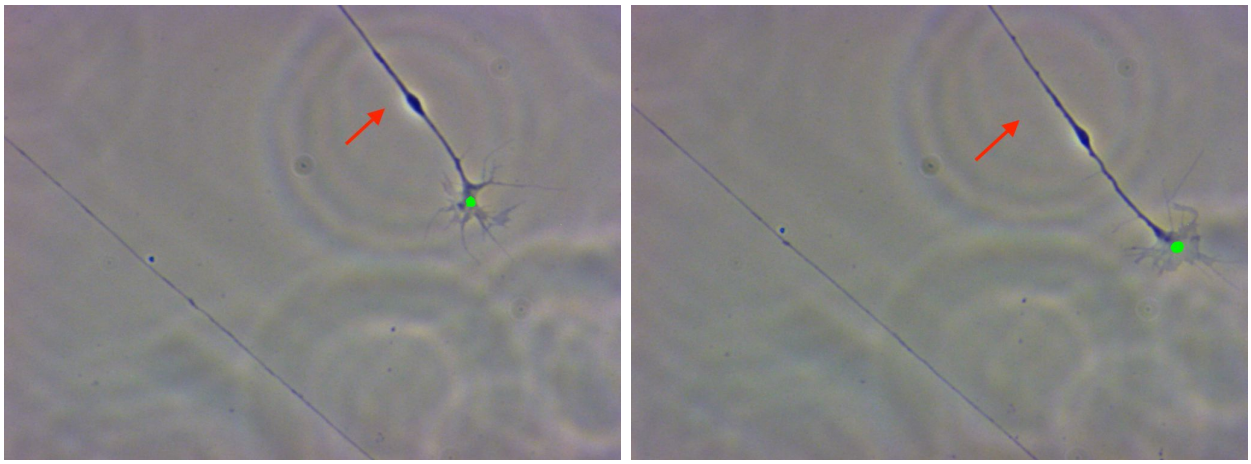

Figure 1: a pair of transmitted light microscopy images comparing an axon in the control condition, marked by the red arrow, from the start of data collection (left) and after 15 minutes of data collection (right). Lamellipod centers are marked by the green dot. Notice the large distance the growth cone was able to travel in only a short amount of time considering the growth cone in the right image has almost moved out of the frame. Image data was collected in collaboration and shared with Cassandra Kennie.

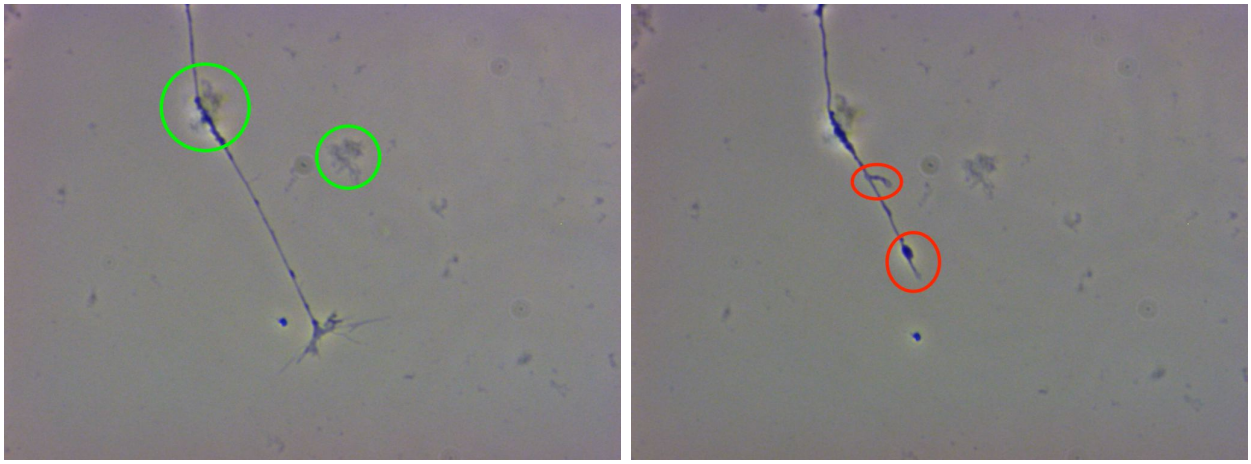

Figure 2: a pair of transmitted light microscopy images displaying a retractile axon in the 2-day amyloid-ß 25-35 level of treatment at the beginning of observation (left) and after 15 minutes (right). Notice the collapse of phase dense structures and loss of linear axonal shape circled in red and large aggregations of protein not found in Figure 1 circled in green. Image data was collected in collaboration and shared with Cassandra Kennie.

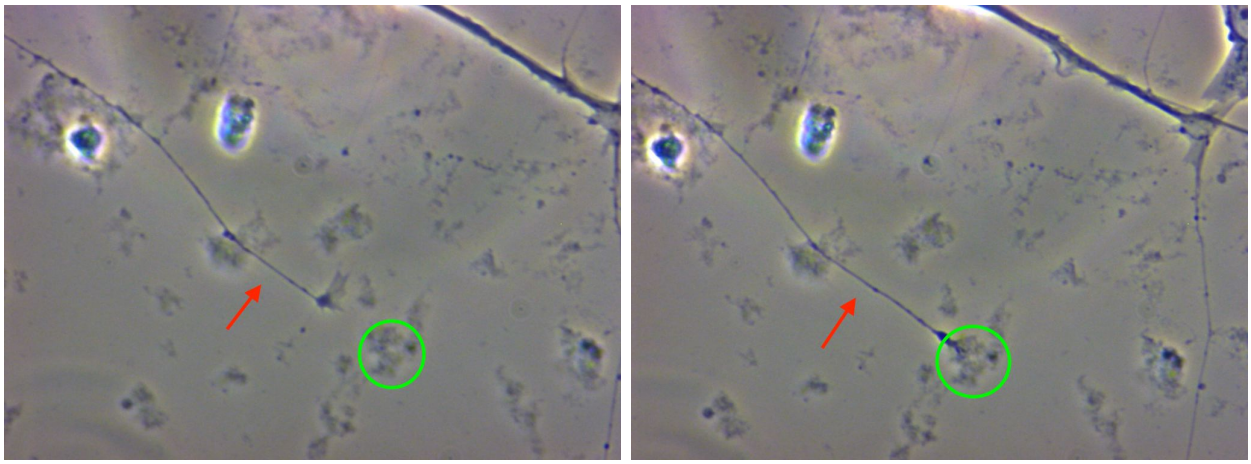

Figure 3: two transmitted light microscopy images showing the growth cone and axon, denoted by the red arrow, of a neuron in the k252a plus amyloid-ß level of treatment at the beginning of observation (left) and after 10 minutes (right). Notice how the axon moves directly into and over one of the amyloid-ß clusters circled in green. Image data was collected in collaboration and shared with Cassandra Kennie.

This data has been quantified in Figure 4 in µm/minute of growth. The value represented by the amyloid-ß and amyloid-ß plus k252a conditions in Figure 4 is an average of the values obtained from each of the two axons measured in those conditions. In the control condition, the axon grew at a rate of 1.597 µm/minute. The axons observed in the amyloid-ß condition displayed retractile action, though by a varying degree as can be seen in Figure 4 with the standard deviation for those measurements. The k252a plus amyloid-ß trial and the control both displayed growth. Considering the control had the highest axonal growth, progressing at a rate of 1.597µm/minute, the k252a and amyloid-ß condition still performed below that of the control group with an average growth rate of 0.917 µm/minute for a difference of 0.680 µm/minute. However, when that difference is compared to the difference between the control and the amyloid-ß 25-35 conditions, the two seem more similar. The average retraction of the axons treated with amyloid-ß was -0.552, despite the high standard deviation, resulting in a difference of 2.149 µm/minute between the two conditions. As both the k252a trial and the control-displayed growth, the amyloid-ß trial deviates from the norm established by the control more than the k252a condition.

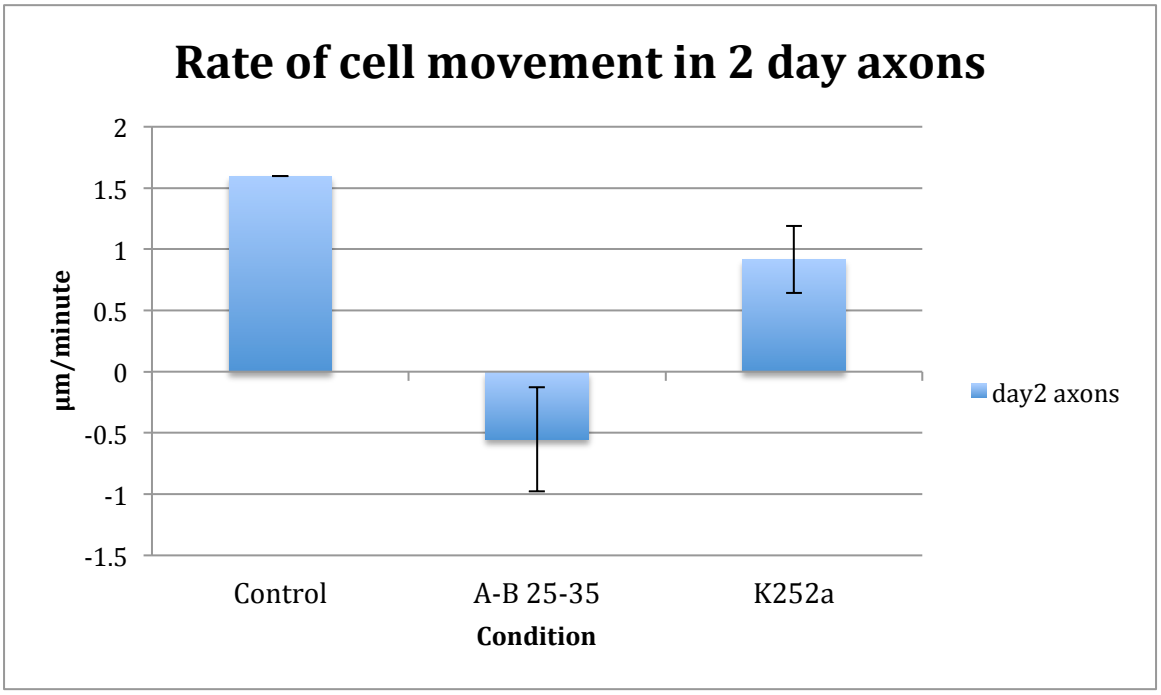

Figure 4: the distance traveled in microns per minute of each growth cone on average. Notice how the amyloid-ß condition has the only negative value despite the high standard deviation of 0.274. The axonal outgrowth in the k252a 2-day trial, while still positive, is less than the control.

Discussion

This preliminary study was to observe potential neurotoxic effects of amyloid-ß fragment 25-35 on axonal outgrowth and, if neurotoxic effects were present, examine effects of kinase inhibitor k252a on cells experiencing neurotoxicity. The results of the study suggest support of the initial hypothesis; the addition of k252a appeared to conserve axonal growth when amyloid-ß 25-35 was present. Since axons began to retract when exposed to exogenous amyloid-ß alone, as

shown in Figures 2 and 4, while no retraction was observed in conditions treated with k252a, the data would suggest that k252a could likely prevent axonal withdrawal. The observed retraction could be explained by a loss of microtubule stability triggering axonal collapse due to amyloid-ß induced activity of kinases affecting tau proteins (Tsai et al., 2004). Additionally, the phase dense structures seen in Figure 2 could be potential signs of destabilized microtubules no longer maintaining linear axonal structure, as retraction does not require complete depolymerization of microtubules to occur (He et al., 2002). A loss of microtubule stability could inhibit distal axon growth and induce retraction (He et al., 2002). Since distal microtubules are inherently less stable, the effects of tau phosphorylation could have been magnified in the distal regions of the axon, which is potentially why axonal retraction was observed in proximity to the growth cone (He et al., 2002; Ikeno and Konishi, 2017). This is supported by the observation that k252a conserved axonal outgrowth and was the primary observed difference between conditions. Since k252a can inhibit kinases associated with tau phosphorylation and can provide overall neuroprotective effects at doss utilized in this and other studies (Roux et al., 2002), this suggests an association between the action of amyloid-ß and k252a (Kase et al., 1987). However, only a correlational relationship between amyloid-ß induced neurotoxicity and neuroprotective k252a is supported by this study.

Because tau phosphorylation was not directly monitored in these cultures, a causal mechanism cannot be established between the neurotoxic effects produced by amyloid-ß fragment 25-35 and kinase inhibitor k252a. While the data support the hypothesis, statistical significance could not be determined due to the modest number of biological replicates. As k252a is a potent kinase inhibitor, nanomolar concentrations are necessary to see neuroprotective effects as opposed to neurotoxic effects with concentrations such as 200nM and 100nM aiding the growth of neurons in culture (Roux et al., 2002). However, the IC50 value for k252a activity on PKC is 32.9nM, which would mean that a concentration of 100nM or greater would potentially completely inhibit the action of the PKC kinase family (Kase et al., 1986). Additionally, k252a acts not just on PKC and PKN or kinases involved in tau phosphorylation, but also acts on cyclic nucleotide dependent kinases like Ca2+/calmodulin-dependent protein kinase II, and thus is likely to have effects on the neurons aside from neuroprotection against amyloid-ß (Hashimoto et al., 1991). K252a also interacts with pathways associated with NGF, which was present in the F-plus medium, so the results from the amyloid-ß and k252a may have been influenced by k252a's inhibitory action on NGF (Cragnolini et al., 2009; Kim et al. 2010). Finally, even though k252a produces neuroprotective effects in dorsal root ganglia of the peripheral nervous system, it shows no increase in long-term survivability of sympathetic ganglia of *Gallus gallus* and it is largely unknown how it would affect central neurons compared to peripheral neurons (Borasio, 1990). These factors can be accounted for in future research as described below.

While the potential neuroprotective effects of k252a on neurons exposed to amyloid-ß 25-35 observed in this study should not be ignored, expanded research is necessary to further support k252a as a treatment for neurodegeneration. Adaptations of the original experiment using neurons of the central nervous system may also provide a more accurate model of Alzheimer's pathology considering k252a does not provide neuroprotective affects to all varieties of neurons (Borasio, 1990). Future studies into the specific action of amyloid-ß are also necessary as the protein fragment induces phospho-activation of several tau-associated kinases such as FYN, PKC, and PKA, but the extent of this activation is largely unknown (Seward et al., 2013). Using a radioactive kinase activity assay, the effects of Amyloid-ß 25-35 on various

kinases associated with tau could be shown, as it has already been shown fragment 25-35 increases PKC activity 1.6-fold on synthetic peptides (Hüll et al., 2006). Further research could utilize that methodology to analyze kinase activity on synthetic peptide regions of tau after exposure to Amyloid-ß 25-35. Additionally, more specific kinase inhibitors could be employed in further studies to mitigate variable kinase inhibition by k252a. Kinases outside of PKN, PKC, or PKA could display greater affinity for k252a, leaving the distribution of its inhibitory effect and uptake into the cell largely unknown (Schneider et al., 2005; Kim et al., 2010). Therefore, a kinase inhibitor with a greater specificity for PKN would be necessary to determine if PKN activity is induced by amyloid-ß 25-35 and if PKN contributes to symptoms of neurodegeneration. Understanding the mechanistic relationship between amyloid-ß aggregate induced kinase activation and NFT formation will become increasingly important in the treatment of Alzheimer's disease as research begins to address the cause, not merely the symptoms, of neurodegeneration.

References

Collaborators:

Stock solutions for amyloid-ß 35-25 and 25-35 were prepared in collaboration with Cassandra Kennie, Ryan McKeon, and Lena O'Flynn. The stock solution for k252a prepared with Cassandra Kennie and Robert Morris. Culture preparation and data collection were performed in collaboration with Cassandra Kennie.

References cited:

Borasio, G. D. "Differential Effects of the Protein Kinase Inhibitor K-252a on the in Vitro Survival of Chick Embryonic Neurons." *Neuroscience Letters*, vol. 108, no. 1–2, Jan. 1990, pp. 207–12.

Brion, J. P. "Neurofibrillary Tangles and Alzheimer's Disease." *European Neurology*, vol. 40, no. 3, Oct. 1998, pp. 130–40.

Burt, D. W. "Emergence of the Chicken as a Model Organism: Implications for Agriculture and Biology." *Poultry Science*, vol. 86, no. 7, July 2007, pp. 1460–71. *academic.oup.com*, doi:10.1093/ps/86.7.1460.

Cragnolini, Andrea B., et al. "Nerve Growth Factor Attenuates Proliferation of Astrocytes via the P75 Neurotrophin Receptor." *Glia*, vol. 57, no. 13, Oct. 2009, pp. 1386–92. *PubMed Central*, doi:10.1002/glia.20857.

Hashimoto, Y., et al. "Potent and Preferential Inhibition of Ca2+/Calmodulin-Dependent Protein Kinase II by K252a and Its Derivative, KT5926." *Biochemical and Biophysical Research Communications*, vol. 181, no. 1, Nov. 1991, pp. 423–29.

He, Yan, et al. "Microtubule Reconfiguration during Axonal Retraction Induced by Nitric Oxide." *Journal of Neuroscience*, vol. 22, no. 14, July 2002, pp. 5982–91.

Hedin, H. L., et al. "Human Platelet Calcium Mobilisation in Response to Beta-Amyloid (25-35): Buffer Dependency and Unchanged Response in Alzheimer's Disease." *Neurochemistry International*, vol. 38, no. 2, Feb. 2001, pp. 145–51.

Hüll, M., et al. "Amyloid Beta Peptide (25-35) Activates Protein Kinase C Leading to Cyclooxygenase-2 Induction and Prostaglandin E2 Release in Primary Midbrain

Astrocytes." *Neurochemistry International*, vol. 48, no. 8, June 2006, pp. 663–72. *europepmc.org*, doi:10.1016/j.neuint.2005.08.013.
Ikeno, Tatsuki, and Yoshiyuki Konishi. "Differential Retraction of Axonal Arbor Terminals Mediated by Microtubule and Kinesin Motor." *Communicative & Integrative Biology*, vol. 10, no. 2, Feb. 2017. *PubMed Central*, doi:10.1080/19420889.2017.1288771.
Kase, H., K. Iwahashi, S. Nakanishi, et al. "K-252 Compounds, Novel and Potent Inhibitors of Protein Kinase C and Cyclic Nucleotide-Dependent Protein Kinases." *Biochemical and Biophysical Research Communications*, vol. 142, no. 2, Jan. 1987, pp. 436–40.
Kase, H., K. Iwahashi, and Y. Matsuda. "K-252a, a Potent Inhibitor of Protein Kinase C from Microbial Origin." *The Journal of Antibiotics*, vol. 39, no. 8, Aug. 1986, pp. 1059–65.
Kawamata, T., et al. "A Protein Kinase, PKN, Accumulates in Alzheimer Neurofibrillary Tangles and Associated Endoplasmic Reticulum-Derived Vesicles and Phosphorylates Tau Protein." *The Journal of Neuroscience: The Official Journal of the Society for Neuroscience*, vol. 18, no. 18, Sept. 1998, pp. 7402–10.
Kim, Chung Kwon, et al. "Neuroprotection Signaling Pathway of Nerve Growth Factor and Brain-Derived Neurotrophic Factor against Staurosporine Induced Apoptosis in Hippocampal H19-7 Cells." *Experimental & Molecular Medicine*, vol. 42, no. 8, July 2010, p. 583. *www.nature.com*, doi:10.3858/emm.2010.42.8.060.
Lattanzio, Francesca, et al. "Treatment with the Neurotoxic Aβ (25–35) Peptide Modulates the Expression of Neuroprotective Factors Pin1, Sirtuin 1, and Brain-Derived Neurotrophic Factor in SH-SY5Y Human Neuroblastoma Cells." *Experimental and Toxicologic Pathology*, vol. 68, no. 5, May 2016, pp. 271–76. *ScienceDirect*, doi:10.1016/j.etp.2016.02.001.
Morris, R.L. (2015a) Neurobiology Bio324 primary culture of chick embryonic peripheral neurons 1: dissection. Accessed 11/20/2017. Available at: http://icuc.wheatoncollege.edu/bio324/2015/NBlabPrimaryTissCultureProc1Dissn2015.htm
Morris, R.L. (2015b) Neurobiology Bio324 primary culture of chick embryonic peripheral neurons 2: observation of live unlabled cells. Accessed 11/20/2017. Available at: http://icuc.wheatoncollege.edu/bio324/2015/NBlabPrimaryTissCultureProc2ObservnOfLliveUnlabeledCells2015.htm
Murphy, M.Paul, and Harry LeVine. "Alzheimer's Disease and the β-Amyloid Peptide." *Journal of Alzheimer's Disease : JAD*, vol. 19, no. 1, Jan. 2010, p. 311. *PubMed Central*, doi:10.3233/JAD-2010-1221.
Perl, Daniel P. "Neuropathology of Alzheimer's Disease." *The Mount Sinai Journal of Medicine, New York*, vol. 77, no. 1, 2010, pp. 32–42. *PubMed Central*, doi:10.1002/msj.20157.
Roux, Philippe P., et al. "K252a and CEP1347 Are Neuroprotective Compounds That Inhibit Mixed-Lineage Kinase-3 and Induce Activation of Akt and ERK." *Journal of Biological Chemistry*, vol. 277, no. 51, Dec. 2002, pp. 49473–80. *www.jbc.org*, doi:10.1074/jbc.M203428200.
Schneider, Tanya L., et al. "Increasing the Kinase Specificity of K252a by Protein Surface Recognition." *Organic Letters*, vol. 7, no. 9, Apr. 2005, pp. 1695–98. *ACS Publications*, doi:10.1021/ol050179o.
Serrano-Pozo, Alberto, et al. "Neuropathological Alterations in Alzheimer Disease." *Cold Spring Harbor Perspectives in Medicine:*, vol. 1, no. 1, Sept. 2011. *PubMed Central*, doi:10.1101/cshperspect.a006189.

Seward, Matthew E., et al. “Amyloid-β Signals through Tau to Drive Ectopic Neuronal Cell Cycle Re-Entry in Alzheimer’s Disease.” *J Cell Sci*, vol. 126, no. 5, Mar. 2013, pp. 1278–86. *jcs.biologists.org*, doi:10.1242/jcs.1125880.

Taniguchi, Taizo, et al. “Phosphorylation of Tau Is Regulated by PKN.” *Journal of Biological Chemistry*, vol. 276, no. 13, Mar. 2001, pp. 10025–31. *www.jbc.org*, doi:10.1074/jbc.M007427200.

Tsai, Julia, et al. “Fibrillar Amyloid Deposition Leads to Local Synaptic Abnormalities and Breakage of Neuronal Branches.” *Nature Neuroscience*, vol. 7, no. 11, Oct. 2004, p. nn1335. *www.nature.com*, doi:10.1038/nn1335.

Zheng, W. H., et al. “Amyloid Beta Peptide Induces Tau Phosphorylation and Loss of Cholinergic Neurons in Rat Primary Septal Cultures.” *Neuroscience*, vol. 115, no. 1, 2002, pp. 201–11.